

# Arginine-Glycine-Aspartic Acid-Conjugated Dendrimer-Modified Quantum Dots for Targeting and Imaging Melanoma

Zhiming Li<sup>1,4</sup>, Peng Huang<sup>2</sup>, Jing Lin<sup>2</sup>, Rong He<sup>2</sup>, Bing Liu<sup>2</sup>, Xiaomin Zhang<sup>3</sup>, Sen Yang<sup>1</sup>, Peng Xi<sup>3</sup>, Xuejun Zhang<sup>1,\*</sup>, Qiushi Ren<sup>1,3,\*</sup>, and Daxiang Cui<sup>2,3,\*</sup>

<sup>1</sup>Institute of Dermatology and Department of Dermatology at No. 1 Hospital, Anhui Medical University, The Key Laboratory of Gene Resource Utilization for Severe Diseases, Ministry of Education, Hefei 230032, China

<sup>2</sup>National Key Laboratory of Nano/Micro Fabrication Technology, Key Laboratory for Thin Film and Microfabrication of Ministry of Education, Institute of Micro-Nano Science and Technology, Shanghai Jiao Tong University, Shanghai 200240, China

<sup>3</sup>Institute for Laser Medicine and Biophotonics, School of Life Sciences and Biotechnology, Shanghai Jiao Tong University, Shanghai 200240, China

<sup>4</sup>Institute of Dermatology and Department of Dermatology at No. 1 Hospital, Wenzhou Medical College, Wenzhou, Zhejiang 325000, China

Angiogenesis is essential for the development of malignant tumors and provides important targets for tumor diagnosis and therapy. Quantum dots have been broadly investigated for their potential application in cancer molecular imaging. In present work, CdSe quantum dots were synthesized, polyamidoamine dendrimers were used to modify surface of quantum dots and improve their solubility in water solution. Then, dendrimer-modified CdSe quantum dots were conjugated with arginine-glycine-aspartic acid (RGD) peptides. These prepared nanoprobe were injected into nude mice loaded with melanoma (A375) tumor xenografts via tail vessels, IVIS imaging system was used to image the targeting and bio-distribution of as-prepared nanoprobe. The dendrimer-modified quantum dots exhibit water-soluble, high quantum yield, and good biocompatibility. RGD-conjugated quantum dots can specifically target human umbilical vein endothelial cells (HUVEC) and A375 melanoma cells, as well as nude mice loaded with A375 melanoma cells. High-performance RGD-conjugated dendrimers modified quantum dot-based nanoprobe have great potential in application such as tumor diagnosis and therapy.

**Keywords:** Melanoma, Quantum Dots, Polyamidoamine Dendrimer, RGD Peptide, Imaging.

## 1. INTRODUCTION

In recent years, molecular imaging of tumors has become a hotspot. However, few reports are closely associated with targeting and imaging melanoma. Melanoma is the third, and most deadly, type of skin cancer, which begins in melanocytes, also can begin in other pigmented tissues such as in the eye or in the intestines.<sup>1</sup> Therefore, to establish the method of targeting and imaging melanoma is very important for melanoma diagnosis and therapy.

In recent years, more and more reports demonstrate that integrin  $\alpha_V\beta_3$  is a very important biomarker, which is only over-expressed in sprouting tumor vessels and most tumor cells such as melanoma, glioblastoma, breast cancer, ovarian cancer and prostate cancers, and plays a critical

role in regulating tumor growth, metastasis and tumor angiogenesis.<sup>2</sup> Therefore, the integrin  $\alpha_V\beta_3$  is considered to be a key receptor for tumor targeting. Moreover, the RGD short peptides can specifically bind with integrin  $\alpha_V\beta_3$ , thus we selected the RGD peptides as the targeting molecules for melanoma targeting and imaging.

Quantum dots (QDs) have been widely studied due to their unique optical properties, and have become a novel functional platform in bio-analytical science and molecular imaging.<sup>3–10</sup> Compared with organic dyes, QDs own marked advantages such as size-tunable emission wavelength and bright stable fluorescence signals. However, some reports showed that QDs exhibit cellular toxicity.<sup>11</sup> How to decrease their toxicity and enhance their biocompatibility is a great challengeable problem.

Dendrimers are a class of polymers with highly ordered structure. The combination of easy functionalization,

\*Authors to whom correspondence should be addressed.

perfect symmetry, nanosize, and internal cavities provide these dendritic nanocomposites with many potential applications in nanomedicine.<sup>12</sup> Dendrimer-coatings of nanoparticle surfaces can alter the charge, functionality, and reactivity, simultaneously also enhance the stability and dispersion of the nanoparticles.<sup>13</sup> Our previous results demonstrate that the dendrimers functionalized nanomaterials such as CNTs, quantum dots and magnetic nanoparticles, markedly enhance the biocompatibility and cellular uptake of nanoparticles.<sup>14–16</sup>

Here we fully used the advantages of RGD, dendrimers and QDs, prepared the RGD-conjugated dendrimer-modified quantum dots nanoprobe (RGD-dQDs), and investigated the feasibility of use of RGD-dQDs as nanoprobe in targeting and imaging melanoma. Our results showed that the as-prepared RGD-dQDs nanoprobe can bind to melanoma cells and vasculature endothelial cells *in vitro*, can also target melanoma *in vivo*. Our studies lay foundation for further clinical application of RGD-dQDs nanoprobe in targeting and imaging melanoma in near future.

## 2. MATERIALS AND METHODS

### 2.1. Synthesis of CdSe QDs

CdSe QDs were synthesized according to our previous reports.<sup>16</sup> Initially, stock selenium solution was prepared by 0.25 mmol selenium mixture with 6.73 mmol trioctylphosphine (TOP). A cadmium stock solution was prepared by heating a mixture of 51.6 g stearic acid and 0.25 mmol cadmium acetate to 260 until a clear, gold-brown solution was obtained. To prepare CdSe QDs solution, the cadmium stock solution was transferred to a 250 ml three-neck round-bottom flask fitted with water cooled condenser and the synthesis was then conducted under a nitrogen atmosphere. The mixture was heated to 260 °C, and the TOPSe solution swiftly injected. The growth temperature was held at 230 °C. The prepared QDs were precipitated by adding methanol into the chloroform solution and isolated by centrifugation at 14,000 rpm and decantation. The resulting wet precipitate was stored for future use.

### 2.2. Preparation of Partially Thiolated Polyamidoamine (PAMAM) Dendrimers

Functional PAMAM dendrimers, with a small number of thiol groups, were prepared by reacting G4.0 amine-terminated PAMAM dendrimers with methyl mercaptoacetate (Alfa Aesar Co.). The synthesis is similar to that described previously.<sup>16,17</sup> All the intermediate products are purified either by ultrafiltration through a 10 K MW cut-off Pellicon device (Millipore Co). The proper amount of methyl mercaptoacetate (NH<sub>2</sub>/SH = 10:1) in methanol was added to 20 mg freshly prepared G4.0 amine-terminated PAMAM dendrimers dissolved in 50 ml of methanol. The

mixture was stirred at 50 °C for 24 hours to obtain functional dendrimers containing some thiol groups. Under vacuum, the solvent was removed at 70 °C to obtain thick, honey-colored oil. The degree of the thiolation and purity of thiolated G4.0 dendrimers were monitored using <sup>1</sup>H nuclear magnetic resonance (<sup>1</sup>H-NMR) (Hitachi H-700H) analysis.

### 2.3. Ligand Replacement and Coating of the QDs

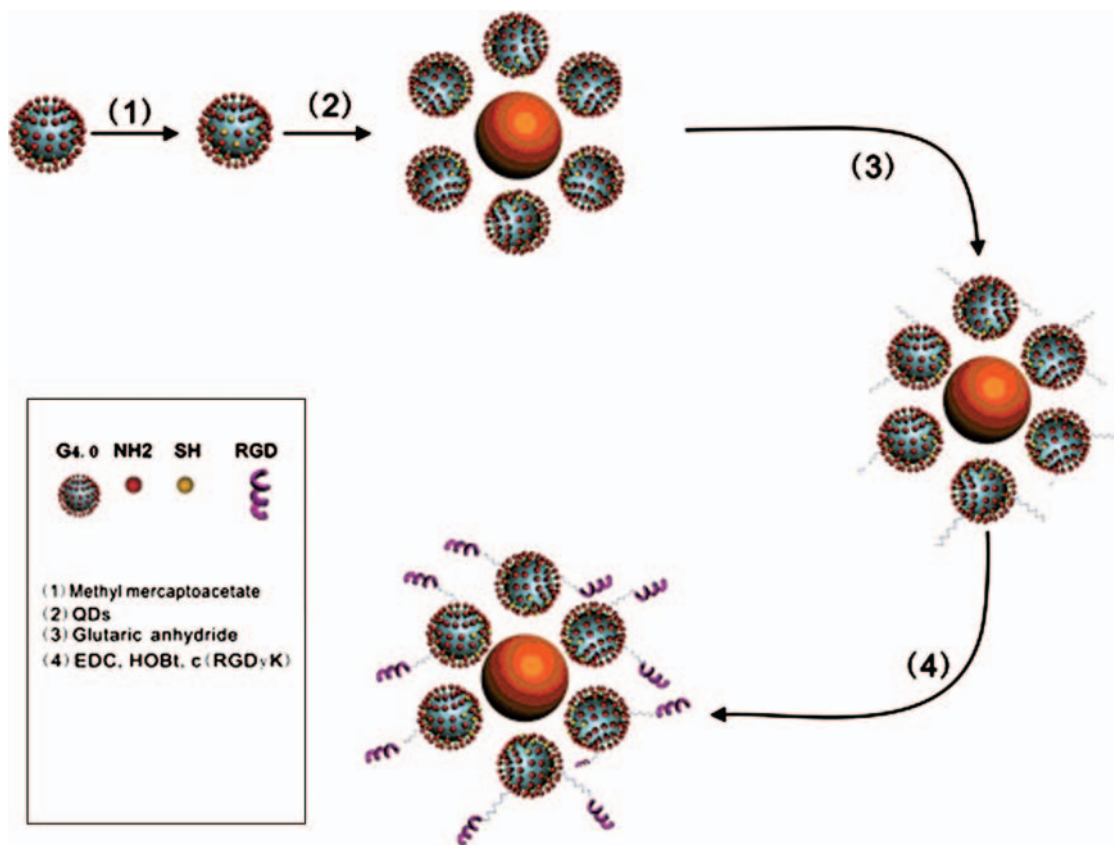
Phase transfer procedure was performed according to previous report.<sup>17</sup> 0.5 ml of thiolated dendrimer in methanol was mixed with 0.5 ml of solution of CdSe QDs in chloroform under argon. Then 1 ml of water was added dropwise until the mixture converted into a stable and two-layered structure. The aqueous layer was removed and the solvent removed under reduced pressure. The QDs were resuspended in a mixture of methanol (0.5 ml) and chloroform (0.5 ml); water was added dropwise until two separate layers formed. The aqueous layer was removed and concentrated under reduced pressure. The resultant solution was transferred into PBS using an ion exchange column.

### 2.4. Bioconjugation of dQDs with RGD Peptides and Their Characterization

Surface amine groups on the surface of dendrimers were converted to carboxylic acids by reacting with excess glutaric anhydride (Alfa Aesar Co.). The conversion procedure is similar to previous reports with some modification,<sup>18</sup> as shown in Scheme 1. Briefly, (1) glutaric anhydride (0.025 mmol) dissolved in 2 ml methanol was added dropwise to a solution of QDs modified with dendrimer (0.00025 mmol) and triethyl amine (Alfa Aesar Co.) (0.025 mmol) in 18 ml methanol while stirring, and the reaction mixture was allowed to stir for another 24 h at room temperature. The solvent was then removed under vacuum, and the residual material was dissolved in H<sub>2</sub>O, purified by extensive ultrafiltration. An active ester was prepared by reacting G4.0 dendrimer-QDs-glutarate in H<sub>2</sub>O with EDC for 4 h. A fifty fold molar excess of RGD (Shanghai Science Peptide Biological Technology Co.) in DMSO (1 ml) was added dropwise to the above solution and allowed to stir overnight. The prepared RGD-dQDs nanoprobe were purified by extensive ultrafiltration against PBS buffer (pH 7.4) and H<sub>2</sub>O, and then lyophilized. The purified nanoprobe were analyzed by high-resolution TEM, <sup>1</sup>H-NMR, fluorescence spectra, and UV-vis spectroscopy. Dynamic light scattering (DLS) was also employed to measure the hydrodynamic diameters of the RGD-dQDs conjugation (Brookhaven 90 plus particle analyzer).

### 2.5. Cytotoxicity of RGD-dQDs Nanoprobes

Cytotoxicity of RGD-dQDs nanoprobe was measured by using the Cell Counting Kit-8 assay (Dojindo



**Scheme 1.** RGD-dQDs conjugation: (1) Firstly prepared partially thiolated PAMAM dendrimers, (2) Partially thiolated PAMAM dendrimers were performed to modify CdSe quantum dots by ligand replacement method, (3) Remain surface amine groups on the dendrimers were converted to carboxylic acids by reacting with excess glutaric anhydride, (4) Finally, the carboxyl groups were activated by reacting with EDC and then conjugated with RGD peptides.

Laboratories). A375, MCF-7 and HUVEC cells were mounted at  $5 \times 10^3$  cells/well in a 96-well plate respectively. After 24 hours of incubation at 37 °C, 100  $\mu$ l DMEM medium containing different concentration of RGD-dQDs nanoprobe (0.001, 0.01, 0.1, 1, 10 nm) was added in each well. The cells were allowed to grow for 24 hours. Evaluation of cell viability through the use of a 10  $\mu$ l Cell Counting Kit-8, after 3 hours incubation, the optical absorbance of the solution was measured at 490 nm using a 96-well microplate reader (Perkin-Elmer).

## 2.6. Expression of $\alpha_v\beta_3$ Integrin of Cells

The breast cancer MCF-7 cell line with lower expression of  $\alpha_v\beta_3$  was selected as a negative control group. Normal human umbilical vein endothelial cells (HUVEC) line and melanoma A375 cell line with over-expression of integrin  $\alpha_v\beta_3$  was selected as the test group. The expression levels of integrin  $\alpha_v\beta_3$  in tumor cells were confirmed by fluorescence activated cell sorting (FACS) (Becton Dickinson). Adherent cells were detached using 0.05% EDTA in PBS for 10 min. Cells were washed in PBS and the pellet carefully resuspended in paraformaldehyde (4%). Monoclonal

integrin  $\alpha_v\beta_3$  antibody (Millipore co) were added to cells in PBS containing 0.5% bovine serum albumin (BSA), and incubated at room temperature for 30 min. Cells were washed twice in PBS. Anti-mouse IgG-FITC (Sigma co.) was added to cells, and incubated at room temperature for 20 min. Cells were washed in PBS and observed by FACS.

## 2.7. Fluorescence Cell Staining and Competitive Cell-Binding Assay

The HUVEC cells, melanoma A375 cells, and MCF-7 were cultured in a DMEM medium supplemented with 10% FBS and 1% penicillin-streptomycin at 37 °C for 2 days. The cells were collected and replated onto 18 mm glass coverslips in a 12-well tissue culture plate and were allowed to grow for 3 days. After rinsing the cells for 3 times, the addition of 500  $\mu$ l of cell-binding buffer, containing different concentration of RGD-dQD nanoprobe to each dish was followed by 30 minutes of incubation. Stained cells were examined under inverted fluorescence microscope (Olympus IX70). Parallel experiments using

pure dQDs and untreated cells were carried out as a control. Before incubation, in order to examine specific binding of RGD-dQD nanoprobe to HUVEC cells and A375 cells, these cells were cultured with free RGD peptides (concentration 1  $\mu\text{M}$ ).

A competitive cell-binding assay on melanoma A375 cells was performed to evaluate the integrin  $\alpha_v\beta_3$  affinity of RGD-dQDs using  $^{125}\text{I}$  echistatin (Amersham co.) (integrin  $\alpha_v\beta_3$  specific).<sup>19</sup> A375 cells were harvested and resuspended in cell-binding buffer.  $1 \times 10^5$  A375 melanoma cells were added in 96-well microtiter plate. 0.02  $\mu\text{Ci}$  of  $^{125}\text{I}$ -echistatin and appropriate volume of the RGD-dQDs solution were added to each well. Adjust the total volume to 200  $\mu\text{l}$  per well with cell-binding buffer and incubate for 2 hours at room temperature. Vacuum manifold was performed to remove the incubation buffer from the 96-well plate. The plates were allowed to dry in the bath incubator and counted in a gamma counter. Each data point is an average of values from triplicate wells. All measurements were repeated three times. The data was fit with a sigmoidal curve using the program Origin 7.5, and the concentration corresponding to 50% bound activity ( $\text{IC}_{50}$ ) was determined.

### 2.8. *In Vivo* Distribution and Tumor Imaging of RGD-dQD Nanoprobe

Animal experiments were performed according to Guidelines for Animal Care and Use Committee, Shanghai Jiao Tong University. Melanoma A375 cells ( $5 \times 10^6$ ) were injected subcutaneously into the right rear flank area of 40 female nude mice with 6 to 8 weeks ages. Tumors were allowed to grow to a diameter of approximately 5 mm. At that point, about 300 pmol of RGD-dQDs nanoprobe in 100  $\mu\text{l}$  PBS was injected into the mice via the tail vein. Mice were respectively sacrificed at 1, 3, 6, and 12 hours. Then, tumor and major organs were removed for histological QDs uptake and distribution studies. Tissue collections were wet weighted, placed on black papers, and subjected to IVIS Lumina imaging.<sup>20</sup> The fluorescence images were acquired, and total fluorescence flux ( $\text{p/s/cm}^2/\text{sr}$ ) for each sample was obtained. Aliquots with known amount of the injection were also put on the black papers and imaged together with the samples. The results were presented as the percentage injected dose per gram (%ID/g).

Melanoma A375 cells ( $5 \times 10^6$ ) were injected subcutaneously into the right rear flank area of nude mice. When the tumor volume reached about 500  $\text{mm}^3$ , the nude mice ( $n = 5$ ) received 300 pmol of RGD-dQDs nanoprobe in 100  $\mu\text{l}$  PBS by tail vein injection. At several time point post-injection, *in vivo* tumor imaging was accomplished using the IVIS Lumina imaging system (Xenogen). For the control experiment, mice ( $n = 5$ ) were injected via tail vein with 300 pmol dQDs nanoprobe and subjected to

optical imaging at various time points post-injection. For the blocking experiment, mice ( $n = 5$ ) were injected with the mixture of 0.5 mg RGD peptides and 300 pmol RGD-dQDs nanoprobe. All *in vivo* images were acquired using 1 s exposure time.

### 2.9. Fluorescence Microscopy and Immunostaining

The mice in test group were euthanized after *in vivo* imaging. The tumor were dissected, cryosectioned into sections 5–10  $\mu\text{m}$  thick, fixed with acetone at 0  $^\circ\text{C}$ , used for fluorescence examination under inverted fluorescence microscope and immunohistochemical study with monoclonal S-100 antibody.<sup>21</sup>

## 3. RESULTS AND DISCUSSION

### 3.1. Characterization of RGD-Conjugated QD Nanoprobe

As shown in Figure 1(a), the synthesized CdSe QDs are about 5–6 nm in diameters, Figure 1(b) showed the HR-TEM images of RGD-dQDs nanoprobe, as-prepared RGD-dQDs nanoprobe exhibited good dispersibility. The measured hydrodynamic diameters of RGD-dQDs nanoprobe are  $13.5 \pm 4.3$  nm, which fits well with in the predicted size (diameter of G4.0 is about 3.5 nm). We calculated the over hydrodynamic diameters (HD) assuming the dendrimers coating adds 3–4 nm organic shell. As shown in Figure 1(c), UV-vis absorption spectra of dQDs and RGD-dQDs are different from QDs. As shown in Figure 1(d), dendrimer-modified QDs decreased the fluorescent intensity of QDs, RGD-conjugated dendrimer-modified QDs also decreased the photoluminescent intensity of QDs.

The conjugate synthesis and characterization were performed using  $^1\text{H}$  NMR spectroscopy. G4.0 PAMAM (300 MHz,  $d^6$ -DMSO):  $\delta = 7.96$  (br s, 60H), 3.08 (br s, 324H), 2.68–2.42 (br s, 160H), 2.20 (br s, 64H). Compared with G4.0 PAMAM dendrimer, partially thiolated G4.0 PAMAM dendrimers shows a distinct signal at  $\delta$  3.74 ppm and 3.66 ppm resulting from  $(-\text{C}(\text{O})\text{CH}_2\text{SH})$  and  $(-\text{NHCH}_2\text{CH}_2\text{NHC}(\text{O})\text{CH}_2\text{SH})$ , respectively. The RGD-dQDs nanoprobe shows signal in the aromatic region for phenyl ring of the RGD peptide ( $\delta$  7.38 and 6.95 ppm).  $^1\text{H}$  NMR spectrum clearly indicates that our RGD peptide conjugated with G4.0 PAMAM dendrimers successfully.

### 3.2. Cytotoxic Analysis of as-Prepared Nanoprobe and Targeting Analysis

As shown in Supplementary Figure S1, RGD-dQDs nanoprobe did not show cytotoxicity within 10 nM. In this study, we used 300 pmol RGD-dQDs nanoprobe to

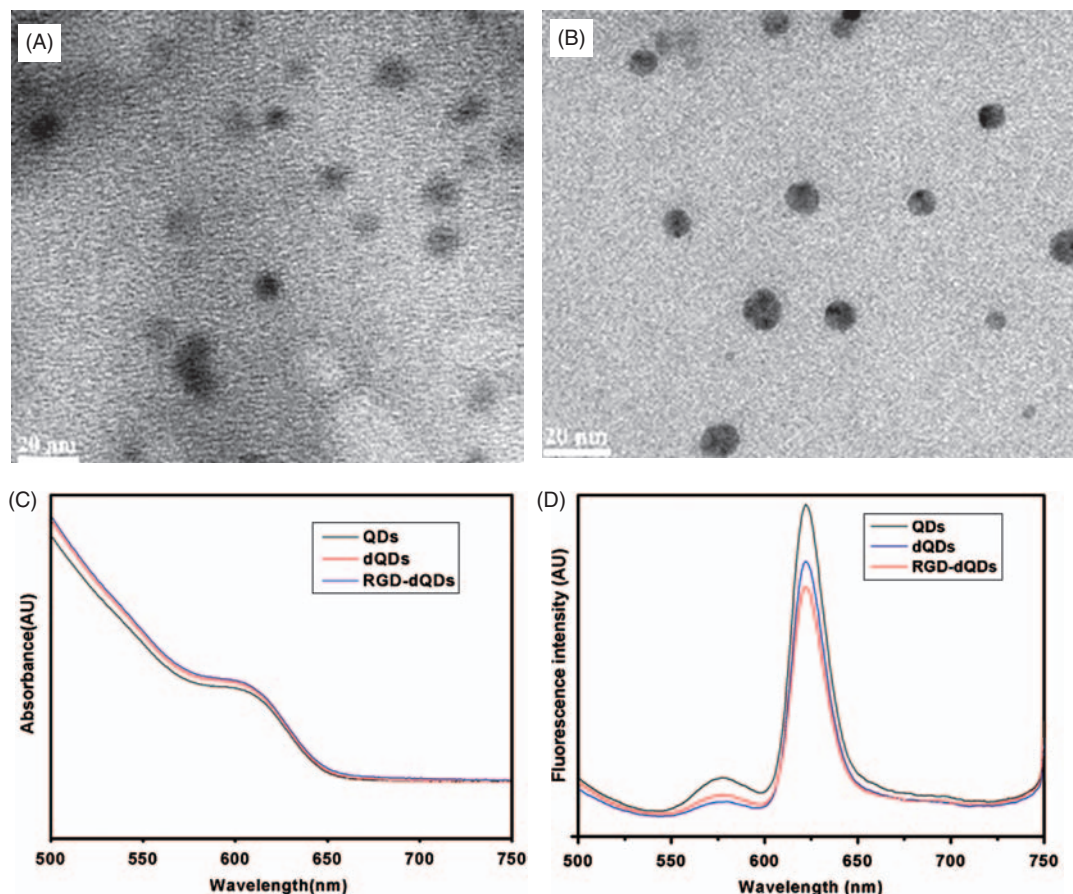


**Fig. 1.** Characterization of QDs, dQDs, and RGD-dQDs. (A) HR-TEM images of QDs. (B) HR-TEM images of RGD-dQDs. (C) and (D) UV-vis absorbance spectra and Photoluminescence spectra of QDs, dQDs, and RGD-dQDs.

target melanoma, which should be safe for the nude mice loaded with melanoma.

As shown in Figures 2(a) and (b), HUVEC cells and melanoma A375 cells incubated with RGD-dQDs

nanoprobes, exhibit strong red color, and could not be washed away, which suggest that the RGD-dQDs nanoprobes can bind with HUVEC cells and melanoma A375 cells. Conversely, the as-prepared nanoprobes can not

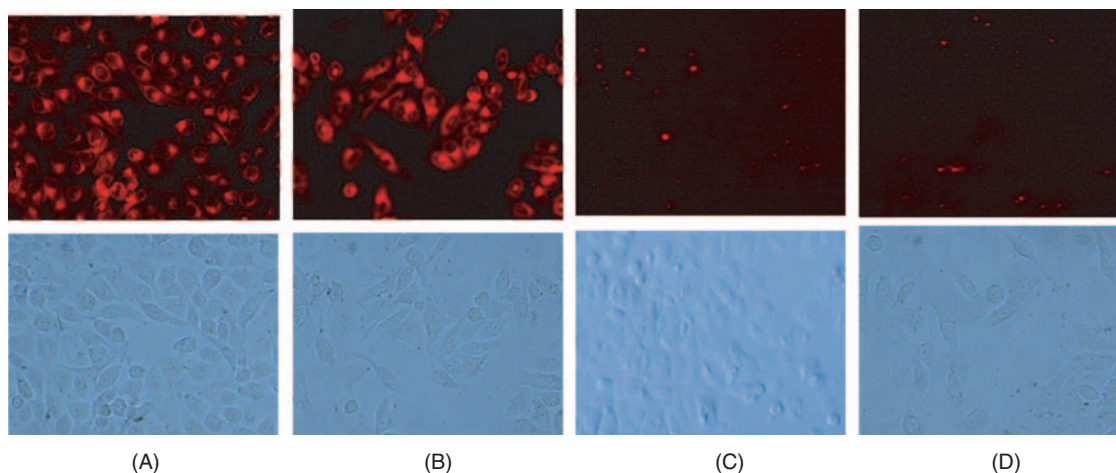


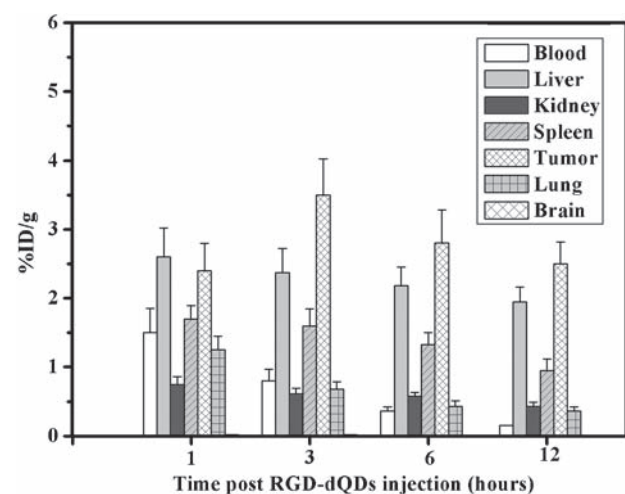
**Fig. 2.** *In vitro* staining of HUVEC, A375, and MCF-7 cells (high and low integrin  $\alpha_v\beta_3$  expression, respectively) using RGD-dQDs nanoprobes. (A) Staining of HUVEC cells with RGD-dQDs nanoprobes. (B) A375 melanoma cells with RGD-dQDs nanoprobes. (C) Staining of MCF-7 breast cancer cells with RGD-dQDs nanoprobes. (D) A375 melanoma cells with dQDs.

bind with MCF-7 cells (Fig. 2(c)) and dQDs can not bind with HUVEC cells and melanoma A375 cells (Fig. 2(d)). Therefore, we considered that RGD-dQDs nanoprobe can target tumor cells with positive expressed  $\alpha_v\beta_3$  specifically. We also observed that the RGD-dQDs nanoprobe inhibited the binding of  $^{125}\text{I}$ -echistatin to A375 melanoma cells in a dose-dependent manner. The 50% inhibitory concentrations ( $\text{IC}_{50}$ ) for RGD-dQDs nanoprobe was 1.752 nM, which highly suggests that RGD-dQD nanoprobe can specifically target  $\alpha_v\beta_3$ -positive melanoma A375 cells (see supplementary data S2).

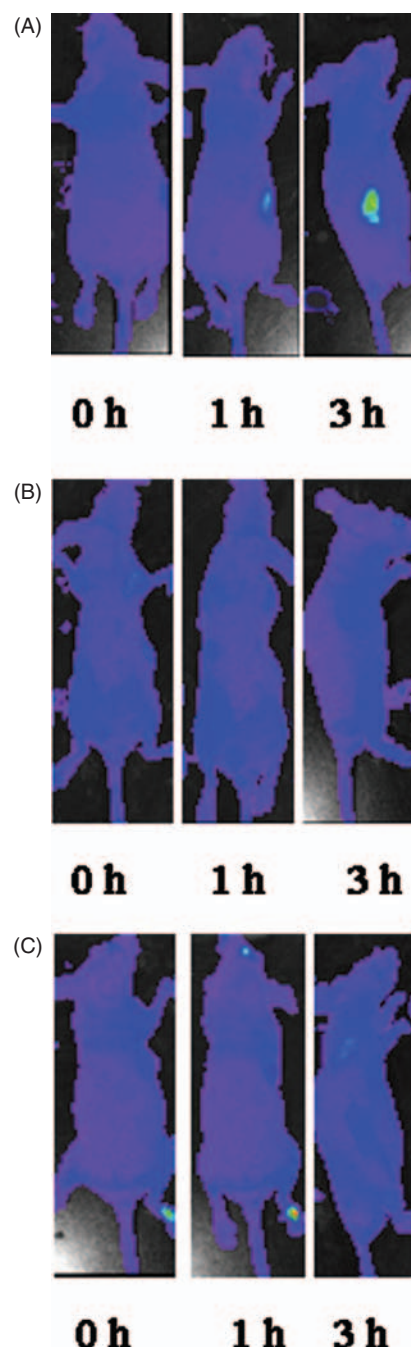
### 3.3. Bio-Distribution of RGD-dQD Nanoprobe and *In Vivo* Imaging in Nude Mice

Figure 3 showed the biodistribution of the prepared nanoprobe in the whole body of nude mice at 1, 3, 6, 12 hours after injection. As the time increased, the amounts of nanoprobe in blood gradually decreased, the amount of nanoprobe in the tumor tissues increased gradually, reach maximal amounts at 3 hours, which suggest the RGD-dQDs nanoprobe can target tumor tissues. We also observed that RGD-dQDs nanoprobe were absorbed and resorted by liver, lung, kidney, and the spleen, almost no accumulation in the heart or brain tissues. As the time extended, the amount of nanoprobe in important organs such as liver, lung, spleen and kidney also gradually decreased.

As shown in Figure 4(a), at 1 hour post-injection of RGD-dQDs nanoprobe, the nanoprobe was observed to locate in the melanoma tissues, as the time increased, the fluorescent signal intensity in tumor sites became more and more strong. As shown in Figure 4(b), the mice in control group1, the fluorescent signals could not be observed,



**Fig. 3.** Biodistribution of RGD-dQDs nanoprobe in nude mice bearing melanoma. Data show RGD-dQDs nanoprobe mainly distributed in tumor, liver, spleen, kidney, and lung throughout the experimental period. Data represent mean values ( $n = 10$ ), bars represent standard deviations for means.



**Fig. 4.** Fluorescent images of nude mice bearing A375 melanoma xenografts at 0, 1, 3 hours post-injection under different condition. (A) The images of mice in test group at 0, 1, 3 hour post-injection of 300 pmol RGD-dQDs nanoprobe. (B) The images of mice in control group1 at 0, 1, 3 hours post-injection of mixture of 0.5 mg RGD peptides and 300 pmol RGD-dQDs nanoprobe. (C) The images of mice in control group2 at 0, 1, 3 hours after injection of 300 pmol dQDs. IVIS Lumina system with a customized filter set (excitation = 500–550 nm, emission = 575–650 nm) was used in this study.

which demonstrates that free RGD peptide can bind with integrin  $\alpha_v\beta_3$  on the surface of melanoma, and blocked the binding of RGD-dQDs nanoprobe with the tumor cells. As shown in Figure 4(c), at 0, 1, 3 hours after injection of

dQDs, no significant fluorescence signal was observed in the site of tumor, which highly suggests that the dQDs do not have the capacity of passive targeting.

### 3.4. Fluorescence Microscopy Observation and Immunohistochemical Staining Analysis

As shown in Figure 5(b), the tumor tissue slices exhibit intensive red fluorescent signals under the fluorescence microscopy, which suggest that the RGD-dQDs nanoprobe entered into melanoma tissues and combined with integrin  $\alpha_V\beta_3$  on the surface of melanoma cells. Figures 5(a) and (c) are the result of H&E staining and immunohistochemical staining analysis, confirming the tumor property is melanoma.

Herein, we used CdSe quantum dots and polyamidoamine dendrimers as raw materials, and fabricated dendrimer-modified CdSe quantum dots, then we selected  $\alpha_V\beta_3$  integrin-over-expressing melanoma cells and tumor vessels as research target, and conjugated dQDs with RGD peptides, the resultant RGD-conjugated dQDs nanoprobe were used to investigate the feasibility of targeting and imaging nude mice loaded with melanoma with the aim of developing a high-efficient QDs-based targeting imaging nanoprobe for early diagnosis of melanoma.

To obtain RGD-conjugated dendrimer-modified QDs nanoprobe, we firstly prepared partially thiolated PAMAM dendrimers, then we used ligand replacement method to obtain partially thiolated PAMAM dendrimers-modified CdSe quantum dots, then, surface amine groups on the surface of dendrimers were converted to carboxylic acids by reacting with excess glutaric anhydride, and then RGD peptides were conjugated with dendrimer-modified QDs, the resultant RGD-dQDs nanoprobe were characterized by HR-TEM, photoluminescence spectra and UV-vis absorption spectra, NMR. Results demonstrated that RGD-dendrimers covered on the surface of QDs, and as-prepared nanoprobe displayed good dispersity and water-solubility, and have strong fluorescent signals.

To evaluate the toxicity of as-prepared nanoprobe, we measured the viability of HUVEC cells, melanoma A375 cells and MCF-7 cells incubated with as-prepared nanoprobe. Results show that as-prepared nanoprobe did not show toxic sign within 10 nM, conversely, pure CdSe QDs markedly decreased cell viability, showing toxic sign. Our results also indirectly showed that RGD peptides and dendrimer molecules can enhance the biocompatibility of CdSe QDs.

To evaluate the targeting of as-prepared nanoprobe, we firstly used FACS to measure the expression levels of  $\alpha_V\beta_3$  integrin in cell lines such as HUVEC cells, melanoma A375 cells and MCF-7 cells (see supplementary data S3), result showed that  $\alpha_V\beta_3$  integrin displayed over-expression in HUVEC cells and melanoma A375 cells, low-expression in MCF-7 cells. These results are consistent with previous reports.<sup>22, 23</sup> Then, we measured the

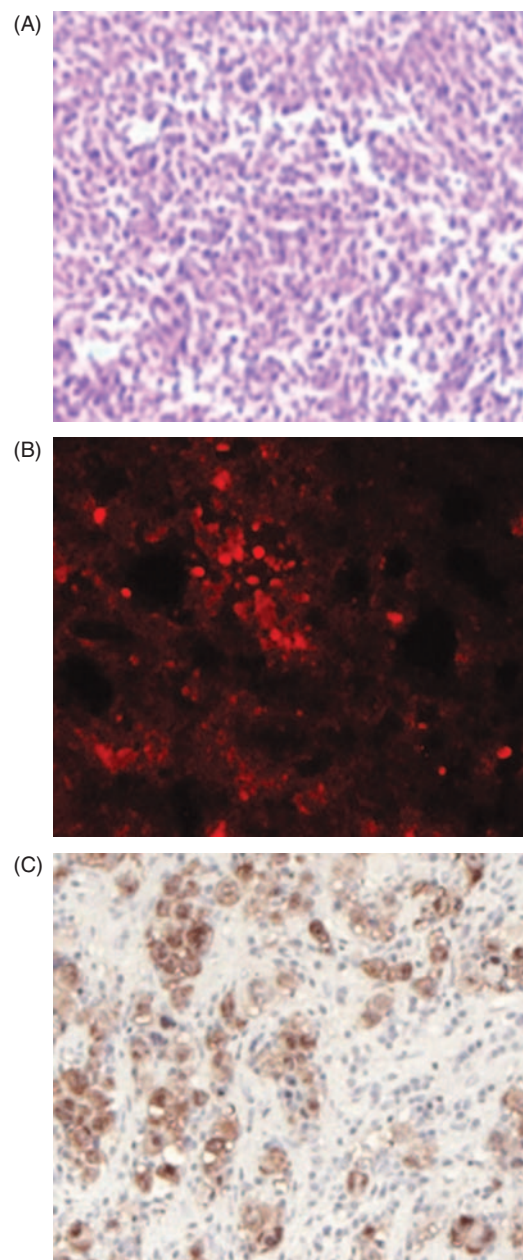


**Fig. 5.** Histologic analysis of A375 melanoma tumor. (A) Tumor tissue H&E staining ( $\times 10$ ). (B) Tumor tissue observation under fluorescence microscope ( $\times 20$ ). (C) Tumor tissue immunohistochemical staining with antibody S-100 ( $\times 10$ ).

binding ability of as-prepared nanoprobe to three kinds of cancer cells, results showed that as-prepared nanoprobe can bind specifically with HUVEC cells and melanoma A375 cells, not bind with MCF-7 cells, competing inhibition test also showed that RGD peptides can block the binding of as-prepared nanoprobe with melanoma A375 cells specifically (see supplementary data S2), therefore, we consider that as-prepared nanoprobe can target specifically melanoma cells.

Previous reports indicated RGD conjugated PEG modified QDs nanoprobes can effectively bind to tumor neovasculature, but do not extravasate.<sup>24,25</sup> Our results showed that, as the time increased, the amounts of nanoprobes in blood gradually decreased, the amount of nanoprobes in the tumor tissues increased gradually, reach maximal amounts at 3 hours, which suggest the RGD-dQDs nanoprobes can target tumor tissues. Compared PEG modified QDs, dendrimer modified QDs could have better ability to permeate cell membranes and enter into cytoplasm since G4.0 PAMAM dendrimers can form nanoscale holes in the surface of tumor cells,<sup>26,27</sup> therefore, RGD-dQDs nanoprobes can extravasate and target melanoma cells.

We also observed that RGD-dQDs nanoprobes were absorbed and resorted by liver, kidney, lung, and the spleen, almost no accumulation in the heart or brain tissues. As the time extended, the amount of nanoprobes in important organs such as liver, lung, spleen and kidney also gradually decreased, which suggest that hydrophilic dendrimers modified QDs can be cleared through the excreting mechanisms of the body.

In order to further confirm targeting of as-prepared nanoprobes in nude mice model with melanoma, we prepared tumor tissues slices and observed strong red fluorescent signals, which suggest that as-prepared nanoprobes were maintained in the tumor tissues. Conversely, dendrimer-modified QDs and pure QDs can not enter into tumor tissues, as shown in Figures 5(b) and (c), which demonstrate that dQDs and QDs don't have the ability of targeting melanoma.

According to above-mentioned results, we suggest a possible model of RGD-dQDs nanoprobes targeting melanoma. RGD-dQDs nanoprobes enter into blood circulation system by tail vessels, quickly distribute into important organs such as liver, spleen, lung and kidney, simultaneously, partial RGD-dQDs nanoprobes enter into tumor vessels via capillary vessels, the RGD peptides of RGD-dQDs nanoprobes can bind with the  $\alpha_v\beta_3$  integrin molecules on the surface of vasculature endothelial cells specifically, the resultant  $\alpha_v\beta_3$  integrin-RGD-dQDs composites were formed in the tumor vessels, finally resultant RGD-dQDs nanoprobes were kept in the tumor tissues for a longer time, therefore, as-prepared RGD-dQDs nanoprobes can target melanoma.

#### 4. CONCLUSIONS

Our study confirms that the RGD-conjugated dQDs nanoprobes can target melanoma cells and vasculature endothelial cells *in vitro*, and exhibits *in vivo* molecular imaging. Compared with present available reports, RGD-dQDs nanoprobes show low cytotoxicity and high stability in biological environments, has great potential in applications such as *in vitro* and *in vivo* melanoma molecular imaging in near future.

## SUPPLEMENTARY

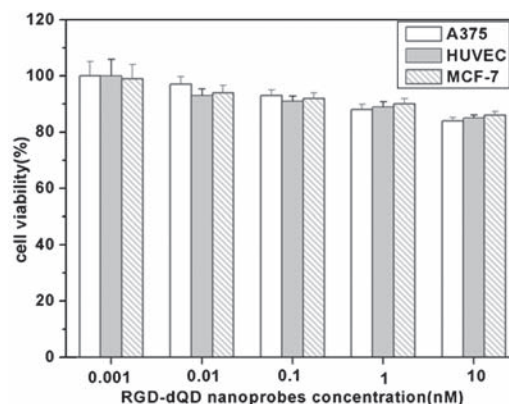


**Fig. S1.** Viability of A375 cells, HUVEC cells and MCF-7 cells after incubation with RGD-dQD nanoprobes. Data represent mean values ( $n = 6$ ), bars represent standard deviations for means.

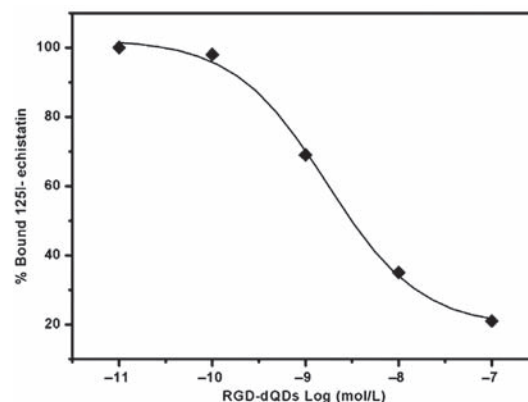


**Fig. S2.** Inhibition of 125I-echistatin (integrin  $\alpha_v\beta_3$ -specific) binding to  $\alpha_v\beta_3$  integrin on melanoma A375 cells by RGD-dQDs.

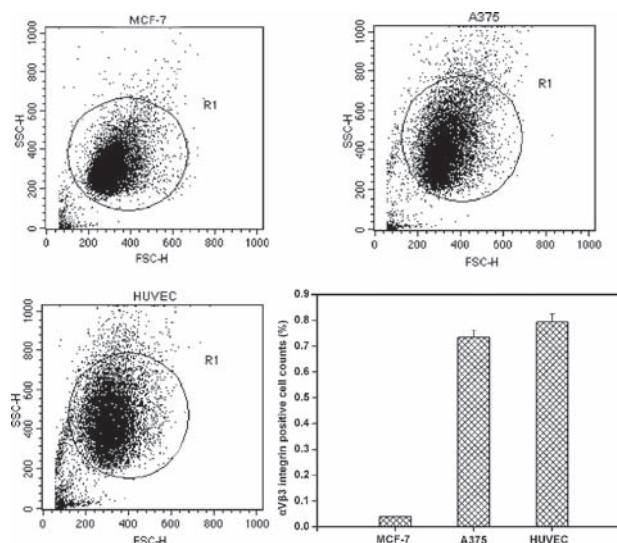


**Fig. S3.** Expression of  $\alpha_v\beta_3$  integrin of MCF-7 cells, A375 cells, and HUVEC cells. Data represent mean values ( $n = 3$ ), bars represent standard deviations for means.

**Acknowledgments:** This work is supported by China National 973 Project (No.2005CB723400-G and 2010CB933901), China National 863 Project (2005AA001070 No. 2007AA022004), National Natural Scientific Fund (No.20471599 and No.30672147), Shanghai Scientific Fund (0752nm24) and Wenzhou Fund of Science and Technology (No.20070034 and No.07211206).

## References and Notes

1. V. Gray-Schopfer, C. Wellbrock, and R. Marais, *Nature* 445, 851 (2007).
2. J. Hood and D. Cheresch, *Nat. Rev. Cancer* 2, 91 (2002).
3. H. Acar, S. Celebi, N. Serttunali, and I. Lieberwirth, *J. Nanosci. Nanotechnol.* 9, 2820 (2009).
4. L. Li, H. Li, D. Chen, H. Liu, F. Tang, Y. Zhang, J. Ren, and Y. Li, *J. Nanosci. Nanotechnol.* 9, 2540 (2009).
5. J. Su, J. Zhang, L. Liu, Y. Huang, and R. Mason, *J. Nanosci. Nanotechnol.* 8, 1174 (2008).
6. S. Toita, U. Hasegawa, H. Koga, I. Sekiya, T. Muneta, and K. Akiyoshi, *J. Nanosci. Nanotechnol.* 8, 2279 (2008).
7. J. Zhang, J. Su, L. Liu, Y. Huang, and R. Mason, *J. Nanosci. Nanotechnol.* 8, 1155 (2008).
8. R. He, X. You, J. Shao, F. Gao, B. Pan, and D. Cui, *Nanotechnology* 18, 315601 (2007).
9. D. Cui, B. Pan, H. Zhang, F. Gao, R. Wu, J. Wang, R. He, and T. Asahi, *Anal. Chem.* 80, 7996 (2008).
10. R. He, D. Cui, and F. Gao, *Mater. Lett.* 63, 1662 (2009).
11. A. Derfus, W. Chan, and S. Bhatia, *Nano Lett.* 4, 11 (2004).
12. C. Lee, J. MacKay, J. Fréchet, and F. Szoka, *Nat. Biotechnol.* 23, 1517 (2005).
13. J. Shan and H. Tenhu, *Chem. Commun.* 44, 4580 (2007).
14. B. Pan, D. Cui, F. Gao, and R. He, *Nanotechnology* 17, 2483 (2006).
15. B. Pan, D. Cui, Y. Sheng, C. Ozkan, F. Gao, R. He, Q. Li, P. Xu, and T. Huang, *Cancer Res.* 67, 8156 (2007).
16. B. Pan, F. Gao, R. He, D. Cui, and Y. Zhang, *J. Colloid Interface Sci.* 297, 151 (2006).
17. A. Wisner, I. Bronstein, and V. Chechik, *Chem. Commun.* 15, 1637 (2006).
18. R. Shukla, T. Thomas, J. Peters, A. Kotlyar, A. Myc, and J. Baker, *Chem. Commun.* 46, 5739 (2005).
19. W. Cai and X. Chen, *Nat. Protoc.* 3, 89 (2008).
20. Z. Cheng, Y. Wu, Z. Xiong, S. Gambhir, and X. Chen, *Bioconjugate Chem.* 16, 1433 (2005).
21. D. Cui, G. Jin, T. Gao, T. Sun, F. Tian, G. Estrada, H. Gao, and A. Sarai, *Cancer Epidemiol. Biomarkers Prev.* 13, 1136 (2004).
22. R. Allman, P. Cowburn, and M. Mason, *Eur. J. Cancer* 36, 410 (2000).
23. T. Byzova, W. Kim, R. Midura, and E. Plow, *Exp. Cell Res.* 254, 299 (2000).
24. W. Cai, D. Shin, K. Chen, O. Gheysens, Q. Cao, S. Wang, S. Gambhir, and X. Chen, *Nano Lett.* 6, 669 (2006).
25. B. Smith, Z. Cheng, A. De, A. Koh, R. Sinclair, and S. Gambhir, *Nano Lett.* 8, 2599 (2008).
26. A. Mecke, S. Uppuluri, T. Sassanella, D. Lee, A. Ramamoorthy, J. Baker, Jr., B. Orr, and H. Banaszak, *Chem. Phys. Lipids* 132, 3 (2004).
27. S. Hong, A. Bielinska, A. Mecke, B. Keszler, J. Beals, X. Shi, L. Balogh, B. Orr, J. Baker, Jr., and H. Banaszak, *Bioconjugate Chem.* 15, 774 (2004).

Received: 15 June 2009. Accepted: 22 July 2009.